H. Bohlen

J. Greschner

J. Keyser

W. Kulcke

P. Nehmiz

# Electron-Beam Proximity Printing—A New High-Speed Lithography Method for Submicron Structures

A laboratory prototype of an electron-beam proximity printer is described which shadow-projects patterns of chip-size transmission masks onto wafers. Electron-beam transmission masks with physical holes at transparent areas have been fabricated with the smallest structures down to 0.3 µm. Experiments to replicate mask patterns were directed at demonstrating the applicability of this lithographic method to high-speed printing of repetitive patterns on wafers. Linewidth resolution and positional accuracy, as well as exposure speed, meet the requirements for micron and submicron lithography.

## Introduction

Over the more than twenty years of integrated circuit development, the functional complexity of circuits has increased each year by a factor of two. As a result of this, the cost of computers has decreased, and their performance has increased in a similar proportion. It is expected that this trend will continue at about the same rate, at least up to the end of the present decade. In the course of this development, improved lithographic techniques have played a major role. Thus circuit components could be fabricated relatively inexpensively with smaller geometries, resulting in reduced propagation delay and power consumption per circuit. But further progress in lithography is required to maintain the performance improvements for future computer generations. At the present time, photolithography is operating near the limits of linewidth resolution set by diffraction effects of the radiation used. Consequently, radiation with shorter wavelengths, such as electron and ion beams and x-rays, is being investigated extensively for future lithographic applications. Aside from improved resolution, positional accuracy of the patterns will become more critical for the finer lines planned for the future. Another requirement is that the lithography costs per pattern element should not exceed the present

Scanning electron-beam systems have been developed, and they already work in production environments [1-3]. They fulfill the stringent requirements of the next generation of lithography. Due to the serial nature of beam-writing, these systems are very flexible with regard to pattern generation (personalization). This flexibility, however, is paid for by limited throughput and high printing costs. For these two reasons, projection systems are better suited to high-volume production.

Projection systems are characterized by their parallel imaging of large mask patterns onto wafers. In photolithographic projection systems this is achieved through the aid of lens or mirror optics. Electron projection systems typically employ electron-optic lenses [4, 5] to transfer the mask patterns onto the wafers. The simplest projection method, however, is that of shadow-imaging. This method does not require an imaging lens system with its associated distortions. Optical shadow-projection systems, called *proximity* or *off-contact* printers, have always been dominant in photolithography when pattern dimensions were in the 5-µm range. This paper describes an extension of the proximity printing principle wherein electrons are used for illumina-

© Copyright 1982 by International Business Machines Corporation. Copying in printed form for private use is permitted without payment of royalty provided that (1) each reproduction is done without alteration and (2) the *Journal* reference and IBM copyright notice are included on the first page. The title and abstract, but no other portions, of this paper may be copied or distributed royalty free without further permission by computer-based and other information-service systems. Permission to *republish* any other portion of this paper must be obtained from the Editor.

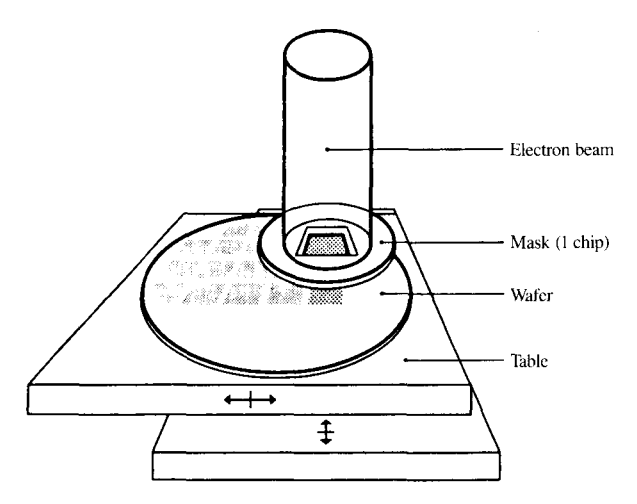


Figure 1 Principle of electron-beam proximity printing.

tion. Electron beams can easily be produced at high intensities. Techniques to handle such beams are well known and the problems associated with fine-line lithography, e.g., pattern registration, have also been solved.

# Electron-beam proximity printing concepts

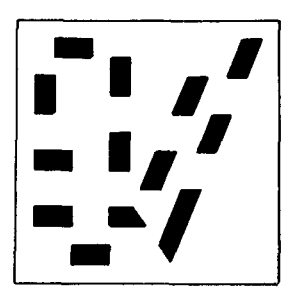
## Principles

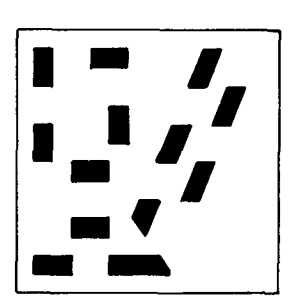
The basic principle is to illuminate a mask with an electron beam to get a shadow image of the transparent mask areas on the underlying wafer (Fig. 1). In contrast to optical proximity printing, where the full wafer is exposed at one time, the mask for electron-beam exposure contains only one or a few chip patterns, so that the entire wafer must be exposed in a step-and-repeat mode. The restriction to a small mask area helps to meet the tight overlay requirements of micron and submicron lithography and facilitates the mask fabrication and inspection process.

Another difference involves the mask itself. Since electrons interact very strongly with matter, a mask for this technique must have physical holes in the transparent areas. Associated with such mask holes is the mask stencil problem. Ring-shaped structures, for example, cannot support their centers. A solution to this problem is shown in Fig. 2. The pattern is divided into small elements which are allotted to two complementary (half) masks. These two masks are arranged side by side on the same mask substrate. The distance between complementary masks corresponds to the distance of the chips on the wafer so that both masks can be printed in one table position.

The distance between the mask and the wafer is about 0.5 mm. It is determined by the beam divergence and defines the depth of focus for this printing method.







Complementary masks

Figure 2 Complementary masks: a pattern is split into elements and shared between two mask areas to overcome the mask-stencil problem.

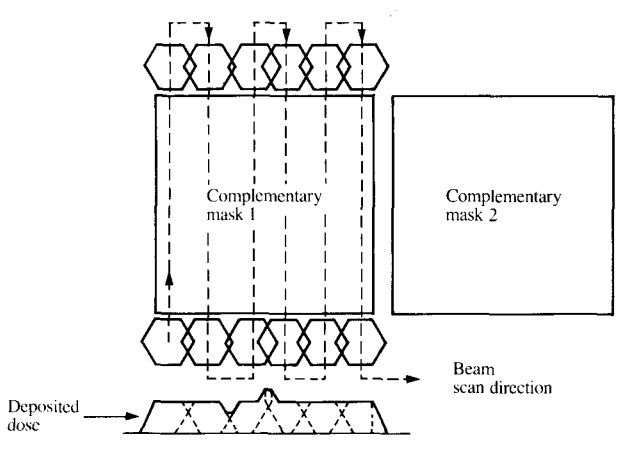


Figure 3 A hexagon-shaped beam is scanned across the mask area for illumination. Small deviations from the nominal scan distances result in negligible variations in the deposited dose.

#### • Mask illumination

Conventionally, a mask is illuminated using a homogeneous floodlight beam which irradiates the whole mask area at one time. The technique chosen here uses a hexagon-shaped electron beam with a "diameter" of about 1 mm. The beam is scanned in a bidirectional manner across the pattern area for consecutive mask illumination. An overlapping of the scans, as indicated in Fig. 3, avoids doubly exposed and unexposed

569

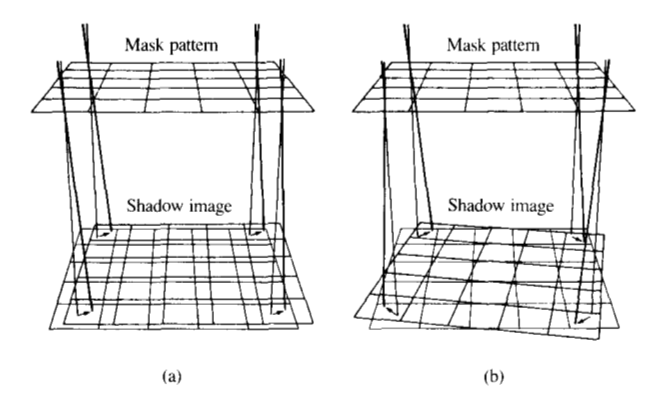


Figure 4 For exact image positioning, beam tilting is employed.

(a) Lateral image shift is obtained through constant beam inclination.

(b) A continuously changing beam inclination results in image rotation.

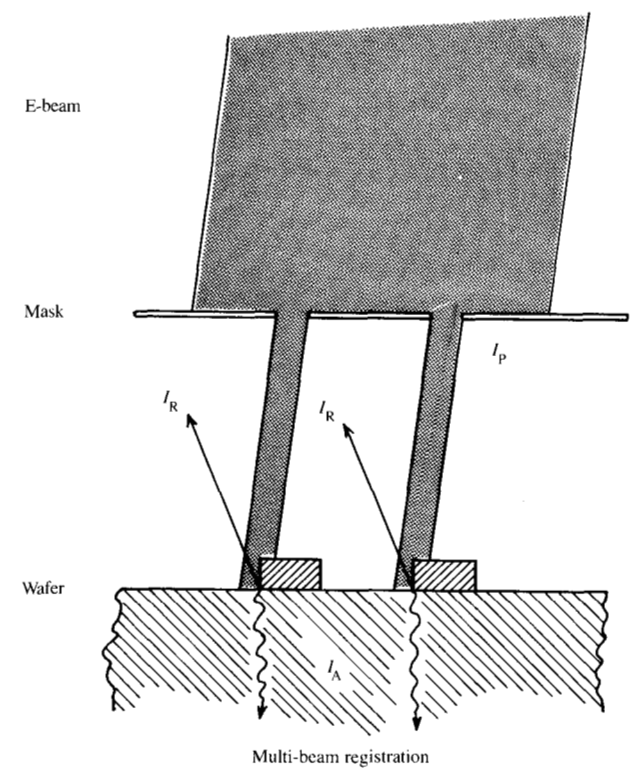


Figure 5 Registration principle: numerous beams are produced through holes in the mask; they are scanned across similarly arranged marks on the wafer; variations in the electron absorbed-beam signal are used to achieve proper registration.

areas if the distances between successive scans differ from their nominal value. Scan errors result in only slight variations of the desired exposure dose.

The small-beam illumination technique (small with respect to the mask size) has the following advantages:

- Different mask sizes can be uniformly illuminated without hardware modifications. Only the scan area has to be adjusted.
- Improved registration signals (compared to flood exposure) can be obtained. The tolerable mask heating during exposure sets an upper limit for the beam current. Concentration of this current into smaller cross sections increases the beam-current density and thus yields stronger registration signals.
- The small-beam illumination offers an additional possibility for rotational image corrections (also discussed further later).
- The equipment can be composed of standard parts already developed for scanning electron-beam systems.

## • Pattern positioning

Level-to-level overlays in submicron lithography and the composition of one chip pattern from two complementary masks require very precise overlays of the mask patterns. In our prototype system the position of the wafer-carrying table is measured with a laser interferometer. When the table is within  $\pm 3~\mu m$  of its nominal position, the exposure cycle can be initiated. The shadow image of the mask is then placed into its exact position by tilting the beam with the pivot point in the mask plane, as illustrated in Fig. 4(a). Due to the large distance between the mask and the wafer (500  $\mu m$ ), a beam tilt of 0.25° already shifts the image about 2  $\mu m$ .

Beam tilting is also used for correcting rotational positioning errors. This correction procedure is illustrated in Fig. 4(b). Since the beam illuminates only a small part of the mask at a time, the image shift can be varied while the beam scans across the mask. Correction signals  $\Delta x(t) = \alpha \cdot y(t)$  and  $\Delta y(t) = -\alpha \cdot x(t)$  are fed to the beam-tilting device and provide an image rotation by an angle  $\alpha$ . The positions of the beam on the mask during scanning are x(t) and y(t). The rotational compensation is restricted to small angles ( $\leq 20$  seconds), since otherwise the pattern would be blurred due to the finite beam diameter.

The rotational correction is used to compensate for table yaw errors and rotational errors originating from imperfect alignment of the wafer on the table with respect to the mask. Information on the table yaw error is obtained from an additional measurement of the laser interferometer. Both types of rotational errors can be kept small so that they are within the correction capability (treated next).

# • Registration

Patterns to be printed on a wafer must be accurately aligned to structures already on the wafer from preceding exposures. The procedure chosen for the electron-beam proximity printer to align the patterns is similar to the technique used in scanning electron-beam exposure systems. Suitable marks on the wafer are scanned with a small electron beam. When

the beam is swept across a mark, a modulation of the backscattered electron signal occurs (Fig. 5). The lateral position of the mark edges can be automatically derived from this signal. The absorbed electron-beam current is used to detect the registration marks, which is equivalent to using the signal from the reflected electrons. Since the incident primary beam current  $I_{\rm P}$  is constant, a change in the backscatter current  $I_{\rm R}$  also affects the absorbed beam current  $I_{\rm A}$  according to the relationships  $I_{\rm P} = I_{\rm R} + I_{\rm A} = {\rm constant}$ , and  $\delta I_{\rm R} = -\delta I_{\rm A}$ .

The small beam required to detect a mark on the wafer is produced by a corresponding hole in the mask. Scanning of such a small beam is achieved by tilting the illuminating beam. Compared to focused-beam systems, this type of electron-beam proximity printing uses a relatively low beam current density. In order to get a strong registration signal, the registration patterns on the wafer and in the mask consist of a large number of squares. Thousands of square beams are thus produced and scanned across suitable marks on the wafer, yielding a strong registration signal.

A typical electron-beam transmission mask contains two registration areas (Fig. 6). One of them carries a pattern used for wafer registration; the other carries a different pattern, to detect the positions of the chips on the wafer. Wafer registration entails two areas on a wafer to be used for detecting lateral and rotational positions with respect to the mask. After the wafer position has been detected by moving the wafer and tilting the beam, the mask is mechanically rotated so that both orientations coincide. Small remaining errors can be compensated for by using the beam rotation method mentioned earlier.

After wafer registration is completed, the wafer may be stepped to the chip positions, which can be accomplished with an accuracy of better than 1  $\mu$ m. The chip registration marks can then be detected by means of beam tilting.

The masks for chip and wafer registration are located beside the two complementary masks, above and below the kerf zone between them. In order to prevent pattern exposure during chip registration, the maximum width of the chip registration area must be smaller than the kerf zone (about  $200-400~\mu m$ ). Its length is equal to the beam diameter (1 mm). Only one registration mark area is required to detect the chip position in x and y.

Although the registration scheme is still under development, we verified that the chip positions can be found with an accuracy of 0.1  $\mu$ m (3 $\sigma$ ). The measurement resolution of the interferometer is 26.4 nm.

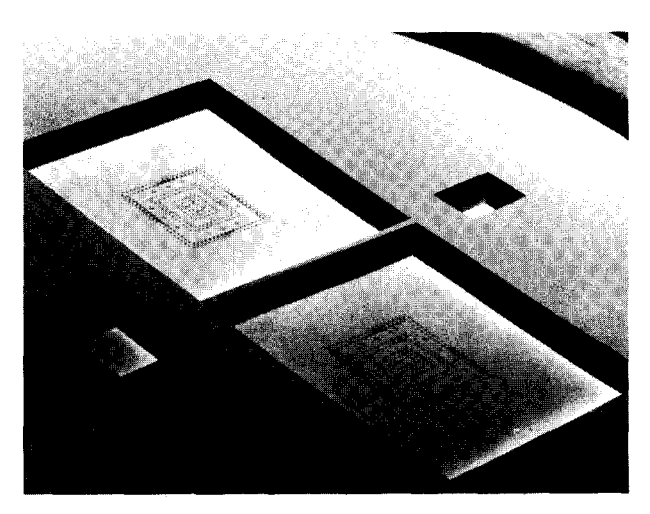


Figure 6 SEM photograph of a transmission mask. The large mask areas  $[(6 \times 6) \text{ mm}^2]$  contain complementary test patterns. The smaller mask areas are used for wafer and chip registration.

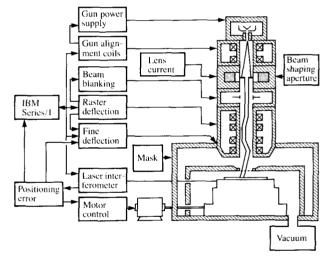


Figure 7 Block diagram of the electron-beam proximity printer.

## **Experimental verification**

A laboratory prototype machine has been built to investigate and demonstrate the fundamental properties of this lithographic method and to develop the lithographic processes for future computer components with submicron structures. The system is shown in schematic block diagram form in Fig. 7.

The column of the system consists mainly of standard parts taken from IBM's scanning exposure system EL-1 [6]. The tungsten hairpin gun produces the beam, which is shaped by a hexagonal aperture inside the collimator lens.

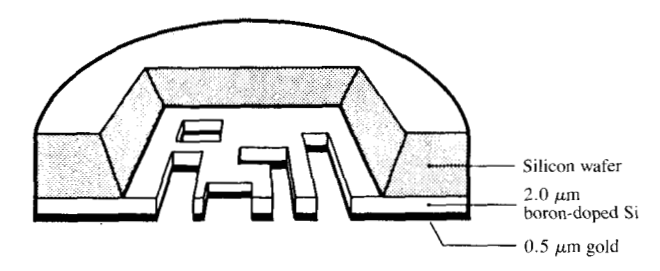


Figure 8 Schematic cross section of an electron-beam transmission mask.

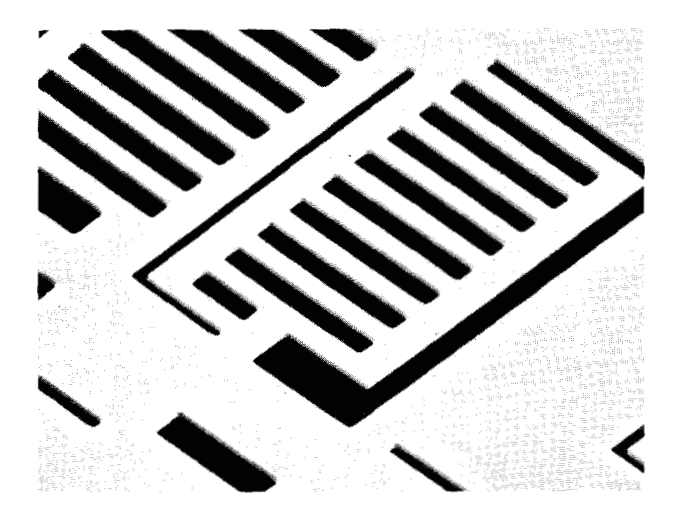


Figure 9 Details of an electron-beam transmission mask. Mask stability is demonstrated with the meander-like pattern elements shown.

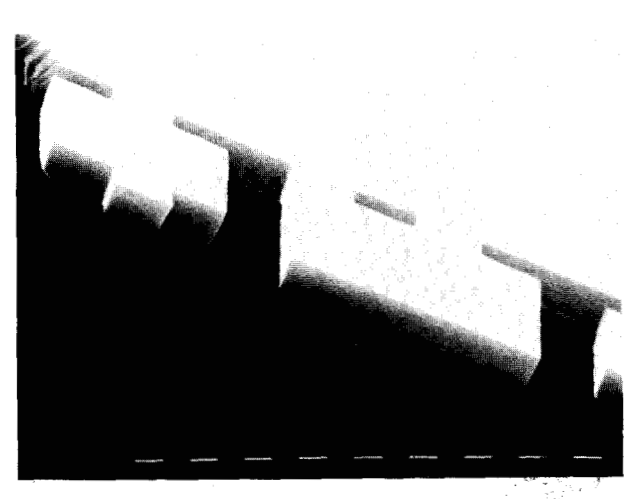


Figure 10 Cross section of an actual electron-beam transmission mask. The SEM photograph shows the vertical profile of the holes. At the bottom of the picture are 1-µm calibration marks.

The alignment section between gun and lens can be used to maintain the beam direction and beam current free of drift during the lifetime of the filament.

Two double-deflection yokes are contained in the lower column section. The upper yokes shift the beam in a raster scan across the mask without changing its inclination. The lower yokes tilt the beam to perform the positional and rotational corrections described earlier.

The vacuum chamber contains the x-y table, the laser interferometer, and the transmission mask supported by a rigid carrier. The column and vacuum chamber are mounted on an air-cushioned mass plate to diminish vibration from the floor.

The basic parts of the electronic control system are the gun power supply for the tungsten hairpin gun, and the gun and brightness servos. The laser interferometer and its electronic circuits determine the position and the yaw of the table. Error signals are derived from these measurements and are fed through a closed-loop system to the fine correction unit for use in beam tilting. The raster scan unit scans the beam across the mask. An IBM Series/1 computer controls the whole system.

# Electron-beam transmission masks

The key part of an electron-beam proximity printer, however, is the transmission mask containing the pattern as  $1 \times$  physical holes. The masks are fabricated from a silicon wafer. The fabrication process is an extension of the familiar x-ray mask process [7, 8]. Additional process steps are used to produce the required holes. Figure 8 shows a schematic cross section of a transmission mask. The basic fabrication steps are as follows:

- The desired pattern is delineated into a resist layer on top of the mask substrate with a scanning electron-beam system.
- After resist development, the pattern is etched into the silicon wafer with vertical walls several μm deep. The etching consists of two reactive ion etching steps in which the first step transfers the pattern from the resist into an intermediate SiO<sub>2</sub> layer and the second step produces the pattern as blind holes in the top surface of the wafer.
- ◆ The wafer is then thinned from the back side using a wet etching process. The thickness of the remaining mask is defined through boron doping of the top surface of the wafer, which acts as an etch stop for this kind of etching process.
- ◆ In a final step, a gold layer is deposited on the mask to increase its heat conductivity and to serve as a beam stop for the high-energy electrons. (More details of the fabrication process have been published in [9].)

Due to the crystalline structure of the thin mask foil, its mechanical stability is excellent. Figure 9 shows meander-like structures contained in a mask. Although they are supported at only two points, they remain flat in the mask plane. It should be mentioned that such complicated structures never occur in a complementary mask set. Here the mask structures are at least 50% solid material, as shown earlier in Fig. 2. This enhances mechanical stability and provides for good heat dissipation. A real cross section of a transmission mask can be seen in Fig. 10, where the vertical profiles of the holes in the foil are clearly visible.

In order to provide for registration of each chip separately, masks are usually made in full chip size [i.e., about  $(5 \times 5)$  mm<sup>2</sup>]. If registration is tolerated for larger areas, masks can be fabricated in larger sizes. Figure 11 is a photograph of a large electron-beam transmission mask containing a semi-conductor pattern 45 mm on a side etched into an 82-mm-diameter wafer.

Electron-beam transmission masks have been fabricated with pattern details as small as  $0.3 \mu m$ . The mask of Fig. 6, which contains  $0.5 \mu m$ -wide lines, was used to create the electron-beam shadow image in poly(methyl methacrylate) (PMMA) resist over a mask wafer distance of 500  $\mu m$ , a portion of which is shown highly magnified in Fig. 12. The jagged edges resemble those of the mask.

# **Proximity effect**

The obstacle to very-fine-line electron-beam lithography is the scattering of electrons in the resist and in the underlying wafer. The beam energy absorbed by a particular shape depends on its size and its position relative to other shapes. This so-called *proximity effect* causes different shapes not to be developed to their designed dimensions despite a uniform exposure. The proximity effect is best observed when a uniformly narrow line has its width affected between sections with and without adjacent lines. However, several schemes are available to reduce this effect in electron-beam proximity printing.

D. F. Kyser and C. H. Ting [10] found that the proximity effect can be reduced through proper choice of the beam acceleration voltage. Exposure experiments with the proximity printer prototype using different voltages confirmed these results. Using 10-keV electrons, proximity effect corrections in 0.9- $\mu$ m-thick PMMA resist are not required for pattern dimensions down to about 0.9  $\mu$ m width. Other correction methods are to preadjust the shape widths properly [11] or to provide additional correction shapes in the complementary mask [12].

The most promising way to curtail the proximity effect, however, is with the use of multilayer resist systems [13]. An

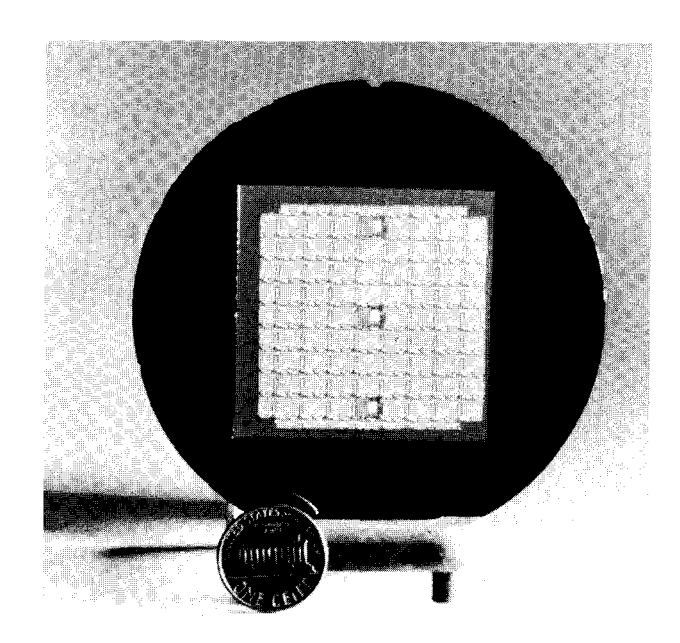


Figure 11 An 82-mm wafer containing a transmission mask measuring 45 mm on a side.

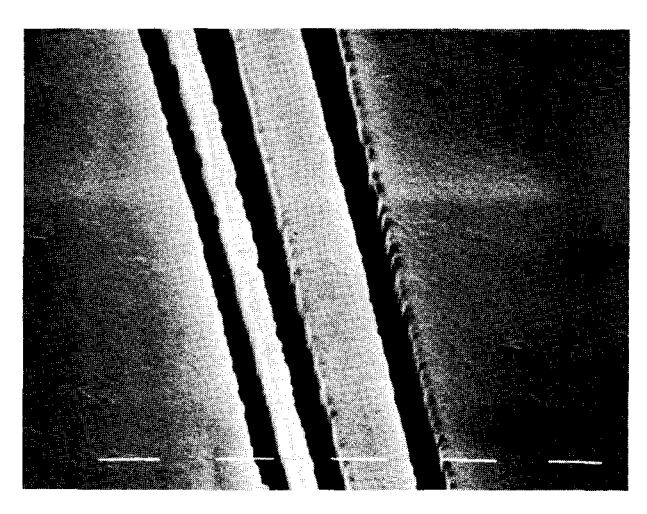


Figure 12 The 0.5- $\mu$ m-wide lines in resist were replicated from a  $1 \times$  mask over a distance of 0.5 mm. At the bottom of the picture are 1- $\mu$ m calibration marks.

example is given in Fig. 13. It shows  $0.6-\mu m$ -wide lines exposed without any proximity effect corrections with 25-keV electrons into a tri-layer resist system. The width of the center line is not affected by the presence or absence of neighboring lines. It indicates that, with the use of multilayer resist systems, the need for proximity corrections may be postponed to lithography applications with lines finer than  $0.5 \ \mu m$ .

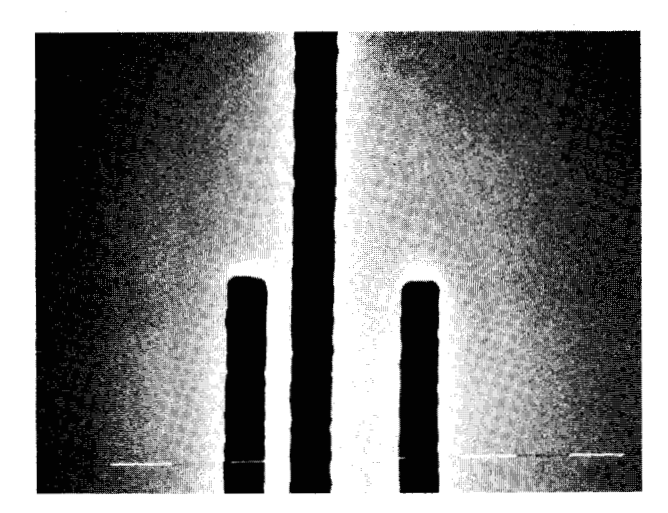


Figure 13 Enlargement showing 0.6- $\mu$ m lines which were exposed at 25 keV into a tri-layer resist without attempts to correct for the proximity effect. At the bottom of the picture are 1- $\mu$ m calibration marks.

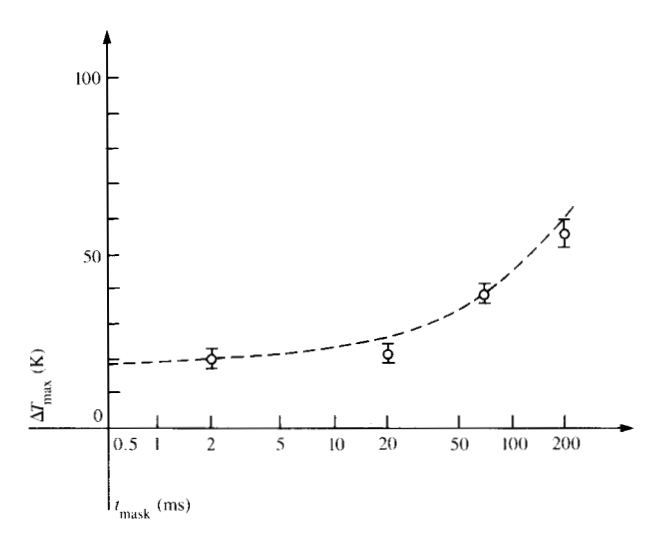


Figure 14 Measured (O) and calculated (---) temperature changes plotted against mask scan time.

# **Exposure speed**

Typical patterns for IC fabrication have a pattern density of 50% or less. In complementary masks, this pattern is distributed over the two mask halves. Consequently, the main portion of the illuminating beam is stopped by the masks during exposure. Absorption of the beam energy causes a temperature increase of the masks, and, potentially, some thermal expansion and loss of pattern fidelity.

In order to find the exposure limits for distortion-free imaging, the temperature rise of the mask center relative to the surrounding frame was determined for constant-dose mask exposures under varying beam-scanning conditions. To that end, a 1-mm-diameter electron beam was scanned across the mask area  $[(5.5 \times 5.5) \text{ mm}^2]$  repeatedly at various scan speeds. In order to maintain the exposure dose constant, the number of mask scans was varied inversely with the time,  $t_{\rm mask}$ , spent for one mask scan. The temperature rise was calculated and also measured with a vacuum-deposited thinfilm thermocouple. A clear correspondence between experimental results and theory was obtained. Figure 14 shows the temperature rise in the mask center for varying exposure conditions. The beam parameters (10  $\mu$ A, 12.5 kV) and the total exposure time (350 ms) were kept constant. The temperature changes were calculated and measured for a silicon mask foil of 2 \mu m thickness with 0.5 \mu m gold on either side. Figure 14 indicates that the lowest temperature rise at the center of the mask is obtained with short scan times, i.e., many mask scans. With mask scan times shorter than 10 ms (corresponding to 35 scans within one exposure), the temperature rise is 20 K and approaches that of a flood exposure of the same dose. Since temperature increases linearly with beam current and beam voltage, the temperature rise can be readily determined for any other beam power.

It has been found that considerable mask heating can be tolerated without introducing distortions. The mask membrane is highly boron-doped as a result of the mask fabrication process. The small boron atoms do not fit perfectly into the silicon lattice and thus cause tensile stress. When the electron beam illuminates the mask, the frame of thick silicon serves as a heat sink. With increasing foil temperature, the thermal expansion increasingly releases the tensile stress. Figure 15 shows that up to a 120 K temperature difference, the mask foil stays flat within its silicon frame. Only above that temperature difference does it start to buckle. In summary, a beam current of about  $60~\mu\text{A}$  can be used at a 10-kV accelerating voltage for mask illumination without overheating and subsequent foil buckling.

Assuming a resist sensitivity of  $5 \mu C/cm^2$ , the exposure time per  $(5 \times 5) mm^2$  chip will be 25 ms. This includes the fact that due to the 1-mm beam diameter, the scan area is larger than the mask area. Twice this time is required when complementary masks are used. Experiments have been made to replicate patterns at an illuminating beam current of  $50 \mu A$ , the present upper limit of the electron-beam gun in the prototype model. This corresponds to an exposure speed of  $4 cm^2/s$  through the two complementary masks. In this regard it should be mentioned that the resist sensitivity is increased by a factor of 2 when the beam acceleration voltage is reduced from 25 kV to 10 kV.

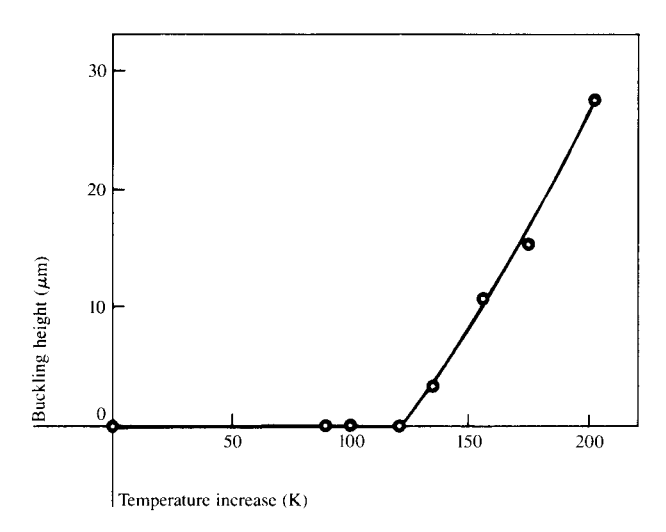


Figure 15 Mask buckling as a function of temperature increase in the center of the mask.



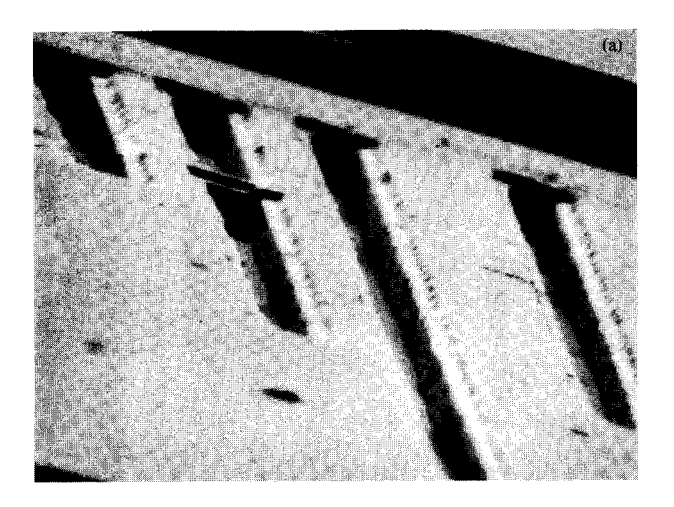
A 10-cm-diameter wafer requires nearly 250 exposures when chip patterns of  $(5 \times 5)$  mm<sup>2</sup> are exposed in a stepand-repeat mode. Therefore masks have to sustain a great number of exposures and yet continue to shape the electron beam uniformly.

Two factors may influence the mask lifetime (printing quality) when the mask is used for a long time. The first factor is a fatigue effect when the mask is repeatedly heated and cooled during the exposure cycles. The second is contamination due to two sources: (1) the hydrocarbons typically found in a vacuum system, which are cracked when they are hit by high-energy electrons, and (2) volatile products released from the resist due to cracking of the macromolecules during the electron-beam exposure. These contaminants can easily reach the mask over the short mask-to-wafer distance of 0.5 mm.

However, experiments have shown that both effects are insignificant. Exposure sequences simulating 200 000 chip images show no differences in image quality within the capabilities of controlling the resist development process. A visual inspection of the mask after the exposure sequence indicates no noticeable contamination layer on the pattern area. Apparently the temperature rise during illumination prevents the contamination from being formed.

# Image positioning

The concept of an exact image placement through beam tilting has been proven as a fast and simple method for



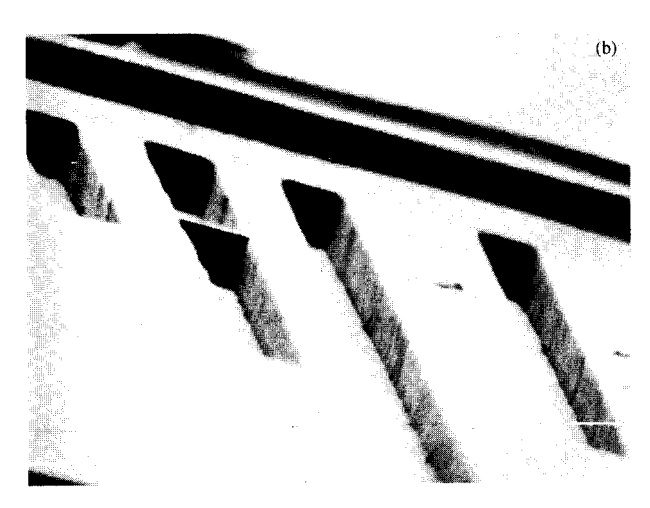


Figure 16 Overlay of two exposures at 50% dose each. (a) Positional inaccuracies not compensated. (b) Positional inaccuracies automatically compensated through beam tilting. At the bottom of the picture are 1-µm calibration marks.

achieving the positioning accuracy required for micron and submicron lithography, especially with the use of complementary masks.

The result is shown in Fig. 16. Figure 16(a) shows the superposition of two exposures of a mask detail with a 50% exposure dose applied to each. The chip site was exposed after the table reached the exposure position from opposite directions. The table positions for the two exposures differed by about 0.5  $\mu$ m. The micrograph indicates that without positional correction through beam tilting the superposition of both exposures is inadequate. In the two 50% dose exposures of Fig. 16(b), the automatic beam-tilting procedure had been used. The difference between the actual and the desired table positions is fed from the laser interferom-

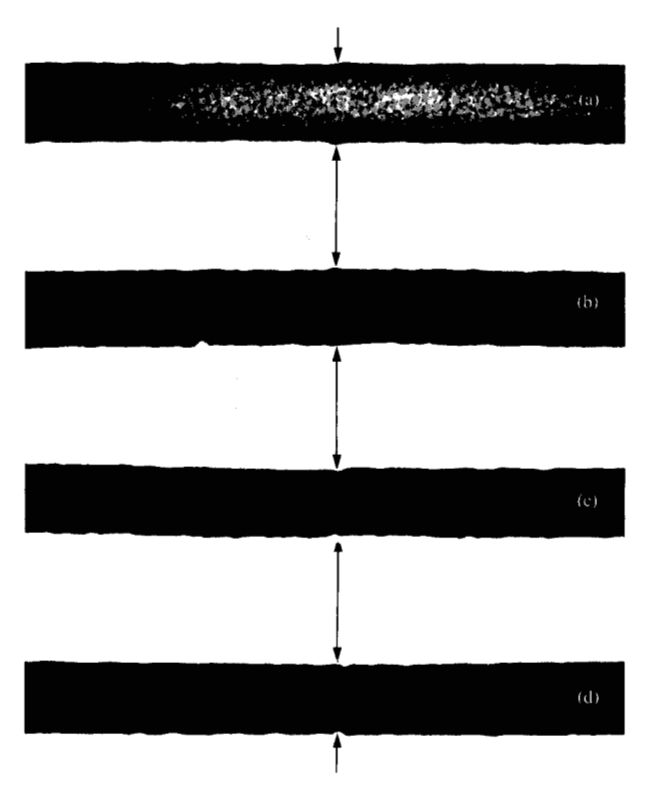


Figure 17 Line-stitching experiments in 1- $\mu$ m-thick PMMA resist. The line ends are moved from overlap (a) to separation (d) in steps of 0.1  $\mu$ m. The butts are indicated by arrows. Best fit is achieved at (b).

eter to the beam-tilting device in a closed loop to compensate for table-positioning errors to better than 0.1  $\mu$ m.

# Complementary mask stitching

The split of a mask pattern into a set of complementary masks is performed by a computer program. Its main ground rules are to avoid ring-shaped structures (the main reason to use such complementary masks), and to avoid long slits, free-standing bars, leaves, etc.

The composition of patterns from two complementary masks requires a very good overlay of the two exposures. This overlay must guarantee that lines which are stitched from parts in complementary masks do not show deficiencies at their butts, *i.e.*, neither constrictions (scalloping) nor protrusions (blooming).

To determine the tolerable stitching distance, colinear lines were printed. In Fig. 17 the distance between the line ends is increased in steps of 0.1  $\mu$ m. Line butt (a) shows a little blooming, indicating an overlap of the line ends. Stitch-

ing is perfect in line butt (b). Line butts (c) and (d) show a slight scalloping. In all cases the effect of stitching, however, is as small as the roughness of the line edges. For practical applications, therefore, the window for complementary mask stitching in 1- $\mu$ m-thick PMMA resist is  $\pm 0.2 \mu$ m around the best butt for a 10-keV electron beam.

Actually achievable overlays of chip-size complementary masks are shown in Fig. 18. This figure is a magnified view of the two overlaid complementary test patterns of Fig. 6. They are printed into PMMA resist on silicon wafers and contain 12 verniers usable for overlay measurements. The vernier increments are 0.1  $\mu$ m; the vernier bars are 2  $\mu$ m wide; the test pattern is  $(1.5 \times 1.5)$  mm²; the center distance of the complementary mask halves is 6 mm. In Fig. 18, the actual locations of the six vernier patterns in the test pattern are shown with arrows. The highly magnified verniers all indicate overlays of 0.1  $\mu$ m or better. This result was verified for 12 verniers on 17 chip sites on three wafers, *i.e.*, a total of 612 vernier evaluations. Not a single vernier displayed an overlay error larger than 0.1  $\mu$ m.

Another line-stitching result is shown in Figs. 19 (a-c). In Figs. 19(a) and (b) the complementary patterns of the number "6" are shown as they appear on the test pattern of Fig. 6. The splitting was overdone on purpose in order to emphasize potential stitching deficiencies. Nevertheless the stitched "6" in Fig. 19(c) shows no scalloping nor blooming.

#### **Throughput**

One of the goals of the work on the electron-beam proximity printer laboratory prototype is to determine the key parameters of this printing method: the cycle times for exposure, registration, and table stepping. From these parameters the throughput for specific applications can be calculated.

The throughput of a typical application may be estimated with the following assumptions: (1) Two sets of complementary masks are used (allowing for a two-chip exposure after each table step). (2) Chip registration is made after every table step in order to compensate for potential wafer distortions. (3) Wafer data and cycle times are taken partially from IBM's EL-3 [14]. By using the values summarized in Table 1, the prorated total time to print one chip is 340 ms. This translates into a throughput of sixty 82-mm-diameter wafers per hour.

#### Conclusions

The availability of a process to fabricate masks with physical holes of submicron precision opens up a new way to produce fine-line lithography with the use of particle beams like electrons or ions. Shadow imaging of such masks eliminates the need for an imaging lens system with its accompanying distortions and associated limits to resolving power.

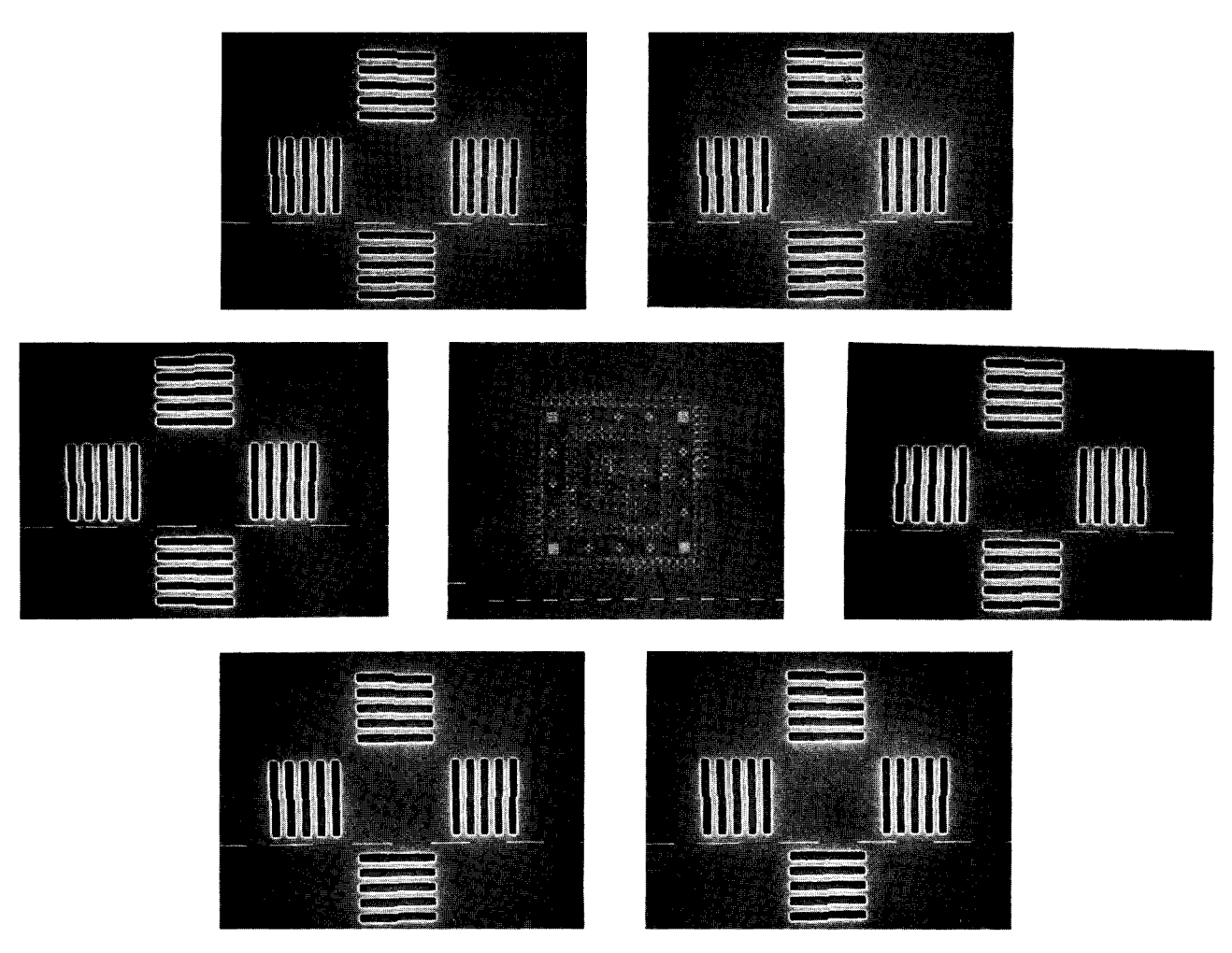


Figure 18 Overlay of complementary test pattern. The entire pattern is shown in the center; arrows mark the verniers shown with higher magnification at the periphery; note 1-µm calibration lines.

An illumination technique using a small hexagon-shaped beam enables standard electron-beam column parts to be used and offers a simple adaptation of the imaging field to arbitrary chip sizes by adjusting the beam-scanned area. In addition, it improves positional accuracy of the printed pattern (lateral and rotary) through beam tilting so that the mechanical movement of the wafer-stepping x-y table can be made coarse and fast, while the precise image positioning is achieved rapidly through electronic means.

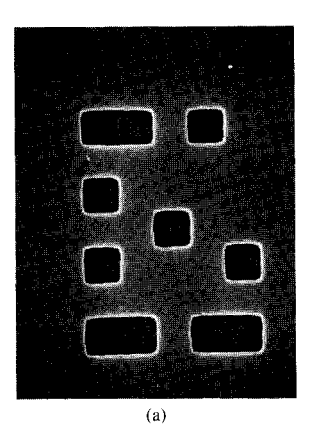
The results obtained so far indicate that all steps for replication of mask patterns can be accomplished very rapidly. A chip exposure goal of 340 ms per chip seems reasonable. This includes complementary mask exposure, table stepping, and chip registration, as well as loading and unloading of the wafer. We therefore conclude that electron-beam proximity printing offers a novel approach to high-speed lithographic printing of micron and submicron patterns for volume production of integrated circuits.

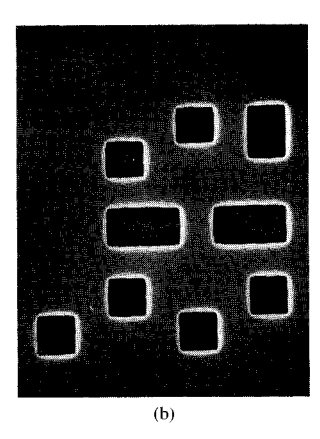
Table 1 Throughput calculation assumptions.

| Wafer diameter   | 82 mm                       |
|--|-----------------------------|
| Chip size  | $(5 \times 5) \text{ mm}^2$ |
| Number of chips on wafer   | 177                         |
| Time required to load/unload/align wafer                                       | 26 s                        |
| Time required to step the table  | 150 ms                      |
| Time required for chip registration  | 100 ms                      |
| Correction factor for stepping to peripheral chip sites and their registration | 1.15                        |
| Exposure time per chip   | 50 ms                       |
| Two chips exposed in one table step  |                             |

# **Acknowledgments**

The authors are pleased to acknowledge many helpful contributions: fabrication of transmission masks was made possible through vector-scan exposures performed by H. Luhn (IBM





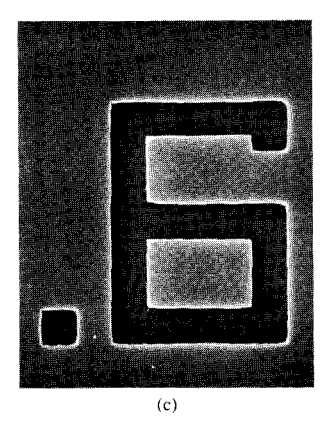


Figure 19 Overlay of complementary test pattern showing the perfect stitching accomplished for the number "6." This is an enlargement taken from an area of Fig. 6; 0.5- $\mu$ m-wide features.

Thomas J. Watson Research Center, Yorktown Heights, NY), and P. Vettiger (IBM Research Laboratory, Zurich); H. J. Trumpp (IBM Development Laboratory, Boeblingen), and B. H. Pogge (IBM General Technology Division facility, East Fishkill, NY) contributed the reactive ion etch processes. W. Recktenwald doped the mask substrates; G. Kraus performed the metal depositions; H. Engelke provided the theoretical evaluations. The building of the laboratory prototype printer was facilitated by H. C. Pfeiffer and W. Stickel (IBM General Technology Division facility, East Fishkill, NY) by furnishing the basic parts for the electron-beam column. M. Kallmeyer developed the electronic control, and K. Asch contributed to the mechanical design.

# References

- R. D. Moore, "Reliability, Availability and Serviceability of Direct Wafer Exposure E-Beam System," Proceedings of the International Conference on Microlithography, Paris, France, 1977, pp. 153-158.
- D. Sofronijevic and A. Oelmann, "One Year E-Beam Mask Making with MEBES—A Users' Report," Proceedings, Microcircuit Engineering '79, Aachen, Germany, 1979, pp. 59-70.

- 3. R. D. Moore, G. A. Caccoma, H. C. Pfeiffer, E. V. Weber, and O. C. Woodward, "EL-3—A High Throughput, High Resolution E-Beam Lithography Tool," J. Vac. Sci. Technol. 19, 950-952 (1981).
- 4. T. P. Chang, M. Hatzakis, A. D. Wilson, and A. N. Broers, "Electron-Beam Lithography Draws a Finer Line," *Electronics* 50, 89-98 (May 12, 1977).
- R. Ward, A. R. Franklin, P. Gould, and M. J. Plummer, "Design and Performance of a Four-Inch Electron-Image Projector," J. Vac. Sci. Technol. 19, 966-970 (1981).
- J. L. Mauer, H. C. Pfeiffer, and W. Stickel, "Electron Optics of an Electron-Beam Lithographic System," IBM J. Res. Develop. 21, 514-521 (1977).
- 7. L. Csepregi and A. Heuberger, "Fabrication of Silicon Oxynitride Masks for X-Ray Lithography," *Proceedings of the 15th Symposium on Electron, Ion and Photon Beam Technology*, Boston, MA, 1979, pp. 1962–1964.
- 8. W. D. Buckley, J. F. Nester, and H. Windischmann, "X-Ray Lithography Mask Technology," J. Electrochem. Soc. 128, 1116-1120 (1981).
- 9. J. Greschner, H. Bohlen, H. Engelke, and P. Nehmiz, "Fabrication Techniques for Electron Beam Transmission Masks," Proceedings of the 9th Symposium on Electron and Ion Beam Science and Technology, St. Louis, MO, 1980, pp. 152-160.
- D. F. Kyser and C. H. Ting, "Voltage Dependence of Proximity Effects in Electron Beam Lithography," J. Vac. Sci. Technol. 16, 1759-1763 (1979).
- M. Parikh, "Calculation of Changes in Pattern Dimensions to Compensate for Proximity Effects in Electron Lithography," Research Report RJ-2463, IBM Thomas J. Watson Research Center, Yorktown Heights, NY, 1979.
- P. Nehmiz, H. Bohlen, J. Greschner, E. Bretscher, and P. Vettiger, "An Approach to Correct the Proximity Effect in Electron Beam Proximity Printing," J. Vac. Sci. Technol. 19, 1291-1295 (1981).
- 13. M. Hatzakis, "Multilayer Resist System for Lithography," Solid State Technol. 24, 74-80 (August, 1981).
- R. Moore, G. Caccoma, H. Pfeiffer, E. Weber, and O. Woodward, "Electron Beam Writes Next Generation IC Patterns," *Electronics* 54, 138-143 (Nov. 3, 1981).

Received July 1, 1981; revised April 26, 1982

Harald Bohlen IBM Germany, P.O. Box 266, 7032 Sindel-fingen, Federal Republic of Germany. Mr. Bohlen joined IBM in 1968 at the German Manufacturing Technology Center. Since then he has worked in the fields of electron-beam machining, inspection, testing, and lithography. Currently he is manager of the Electron Beam Technology Department at the German Manufacturing Technology Center and responsible for the development of electron-beam proximity printing. He holds three IBM Invention Achievement Awards. Mr. Bohlen received his Dipl. Phys. degree from the University of Erlangen, Germany, in 1967. He is a member of the German Physical Society.

Johann Greschner IBM Germany, P.O. Box 266, 7032 Sindelfingen, Federal Republic of Germany. Dr. Greschner is manager of one of the applications departments in the Sindelfingen plant information systems group. Prior to his promotion he was a member of the Electron Beam Technology Department at the German Manufacturing Technology Center, where he engaged in electron-beam lithography. He has been developing electron-beam transmission masks for the new lithographic method of electron-beam proximity printing. He received his degrees of Dipl. Phys. and Dr. rer. nat. from the University of Tuebingen, Germany, and joined the German Manufacturing Technology Center in 1974. Dr. Greschner received an IBM Outstanding Innovation Award and holds three IBM Invention Achievement Awards for disclosures about his work in electron-beam technology, silicon micromechanics, and reactive ion etching.

Joachim H. Keyser IBM Germany, P.O. Box 266, 7032 Sindelfingen, Federal Republic of Germany. Mr. Keyser works in the Electron Beam Technology Department at the German Manufacturing Technology Center. He is responsible for the mechanical development and engineering of the electron-beam proximity printer laboratory prototype. In 1956 he joined IBM at Sindelfingen, where he worked in the product engineering area. He acted as liaison engineer and had the engineering responsibility for various products of the Office Products Division. In this position he worked in Amsterdam, the Netherlands, 1961 to 1962; Lexington, Kentucky, 1964 to 1966; and Berlin, Germany, 1966 to 1967. Prior to his work with the electron-beam group, he worked on unconventional manufacturing methods. Later he covered software problems on several experimental and analysis tools. Mr. Keyser received the B.A. from the Staatliche Ingenieurschule at Esslingen, Germany, in 1956.

Werner Kulcke IBM Germany, P.O. Box 266, 7032 Sindel-fingen, Federal Republic of Germany. Dr. Kulcke is manager of the manufacturing instruments group at the German Manufacturing Technology Center. He is responsible for the development of new processes and tools in electronics, optics, and electron-beam technologies for the fabrication of future computer components. He received the Dipl. Phys. and Dr. rer. nat. degrees from the University of Stuttgart, Germany. Prior to joining IBM, he developed a radio-sonde for measuring the ozone content in the upper atmosphere at

the Max Planck Institute in Weissenau, Germany. From 1956 to 1962, he worked at the IBM Germany research and development laboratory, Boeblingen, with ferroelectric materials, electro-optics, and optical printing. From 1962 to 1966, he was responsible for the development of an electro-optic light deflector at the Data Systems Division development laboratory in Poughkeepsie, New York. He received an IBM Outstanding Achievement Award and holds eleven IBM Invention Achievement Awards. Dr. Kulcke is a member of the German Physical Society for Applied Optics.

**Peter Nehmiz** IBM Germany, P.O. Box 266, 7032 Sindelfingen, Federal Republic of Germany. Since 1974, Dr. Nehmiz has been a member of the Electron Beam Technology Department at the German Manufacturing Technology Center. He is engaged in the development and testing of a laboratory prototype machine for electron-beam proximity printing. He is responsible for all aspects concerning exposure and registration. In 1971 he joined IBM at the research and development laboratory in Boeblingen, Germany, and worked until 1974 as a systems programmer. He received the diploma and the Dr. rer. nat. in physics from the Gutenberg University, Mainz, West Germany. In 1969-1970, he spent a postdoctorate year at the Physical Faculty of the Lomonossow University, Moscow, U.S.S.R., funded by an exchange program between the Deutsche Forschungsgemeinschaft and the Academy of Sciences of the U.S.S.R. Dr. Nehmiz has received two IBM Invention Achievement Awards.